Developing discrete element model of cracking jointed limestone due to blast-stress wave propagation

Asghar Pourih Heegh[1], Arash Refahi[2*], Morteza Hoseini[3]

1- Rock Mechanic Student, Mining Department, Faculty of Engineering, University of Zanjan, Zanjan, Iran. E-mail Address: asgharpourih@yahoo.com

2- Corresponding Author: Assistant Professor, Mining Department, Faculty of Engineering, University of Zanjan, Zanjan, Iran. E-mail Address: refahi.arash@znu.ac.ir

3- Assistant Professor, Mining Department, Faculty of Engineering, University of Zanjan, Zanjan, Iran. E-mail Address: m.hoseini@znu.ac.ir

Abstract

In this study, the effect of joints on rock breakage due to blast stress wave propagation in limestone has been investigated. The required rock strengthh properties were measured from limestone specimens extracted from Angooran lead-zinc mine located in the north-west of Iran. Also, geometrical properties of three joints were given from the benches of mine. The particle flow code in two dimensions (PFC2D) has been used to model applying blast pressure to inner walls of 6 holes; this code was based on discrete element method (DEM). The obtained results showed that producing large pieces of rocks and back-break processes increased by making larger the distance between holes and free surface (B). Also, decreasing B caused to increase the producing powdered limestone around the holes. DEM models confirmed when the stress wave reached empty spaces between joint surfaces, it lost a large part of its energy and the wave passed from the joints could not break limestone well. Furthermore, creating a large number of cracks around the holes showed that the powdered areas started to develop by propagating the stress wave. Comparing the results obtained from DEM models with experimental data showed that the discrete element method was an appropriate method to simulate the rock fracturing process during the blast wave propagation. Also, the blast wave propagation was modeled well in the plane strain condition.

Keywords: Back-break process, Powdered area, Fracture process of rock, Particle flow code, Plane strain

1. Introduction

Blasting is used in the mining and construction industries as the dominant method to break hard rocks. In open pit and underground mines, drilling and blasting are the first stage of production cycles. The results such as rock fragmentation rates, shape of the productions etc. affect subsequent-mining activities. In the process of explosion, the size and amount of broken rock pieces depend on creating and propagating cracks, stress waves produced by the blast pressure and throwing rocks. Badly designing blast patterns in open pit mines causes to crack remaining walls (back-break process), to decrease the stability mine walls and to increase the size of broken pieces [1-5]. Furthermore, the back-break rate depends on structural and mechanical properties of rock mass. Therefore, it is possible to achieve the desirable crushing and reduce the back-break by developing an optimal blasting design [6, 7].

According to several researches, developing an optimal network of fractures requires understanding the mechanism of explosion [8-10]. They have confirmed that some characteristics such as explosive properties [10, 11], strength of rock mass [12, 13], velocity of wave propagation [13], geological structures [14] and stress distributions would remarkably affect on fracture networks [15]. Also, waveform propagation and natural fractures [16], spacing of blast holes [17], hole diameters [18] and pre-existing discontinuities have the most important effects for increasing the smoothness of final wall faces in open-pit mines [19, 20]. A blasting research-subject can be divided into three parts: empirical and semi-empirical techniques, small-scale experiments and numerical simulations. Empirical and semi-empirical techniques, which are based on in-situ information, and small-scale experiments cannot consider geological and explosive conditions. However, numerical methods simulate well explosive damages in rock mass with different geological conditions [20- 23].

The main purpose of this study is to develop a discrete element model (DEM) of cracking rock due to the blast-stress wave propagation and effects of rock structures, in order to investigate a suitable pattern of blast holes for Angooran lead and zinc open-pit mine that is one of the largest metal mines in Iran. It is located in Zanjan province (40° 36´ in longitude and 20° 47´ in latitude of the geographical coordinates) and in a region with an average altitude of 3000 m. The ore body is located between a limestone layer as hanging-wall and on a thick layer of schist as foot-wall. In Angooran mine, rocks in hanging-wall are collections of semi-metamorphic limestone with an approximately 200 m in thickness that the most extension of these collections are in the east of the mine including some joint sets. The required data (i.e. geometrical and mechanical properties of joints and rock) were obtained from surveying mine and previous studies [24, 25].

DEM is a modeling method based on the discontinuum mechanics [26, 27]. In this study, the wave produced by detonating ANFO charge in six blast holes was simulated in intact and jointed limestone by the particle flow code in two dimensions (PFC2D which is based on DEM. It simulated the limestone environment as a granular assembly by gathering many stiff particles bonded together [26, 27]. The previous study confirmed that the stress wave propagation in rocks was well simulated using PFC2D [23]. To verify the obtained results, they have been compared by confirmed data in previous similar studies.

2. Materials and Method

In order to model breaking rocks due to propagate blast wave stresses, the mechanical properties of the limestone specimens were experimentally evaluated. Three stone blocks of limestone were extracted from Angooran mine. Then six cylindrical specimens with 110 mm in height and 54 mm in diameter (Fig. 1) and 6 disc-shape specimens with 54 mm in diameter 27 mm in thickness were prepared from the blocks. A standard uniaxial compressive test and Brazilian test were carried out on the cylindrical and disc-shape specimens, respectively. Furthermore, the dry density of limestone was estimated by the saturation and caliper technique, which was defined by International Society for Rock Mechanics (ISRM). The obtained mean-mechanical properties are shown in Table 1. Geometrical and mechanical properties of three joint sets were extracted by surveying the benches and previous studies [24- 28].

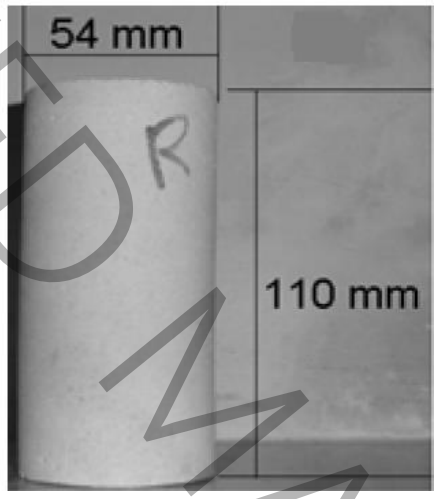

Fig. 1. Cylindrical specimen prepared from Angooran Limestone.

Properties of limestone	
Density	2500 Kg/m^3
Uniaxial compressive strength	39 MPa
Young's modulus	11 GPa
Poisson's ratio	0.18
Tensile strength	5 MPa

Table 1. Properties of Angooran limestone

	First joint set	Second joint set	Third joint set
Cohesion	0	0	0
Friction angle	33°	33°	33°
Average joint spacing	1.5 m	3 m	2 m
Average joint separation	2 mm	3.5 mm	6.5 mm
Average Azimuth angle of joint dip direction	7°	125°	15°

Table 2. Geometrical and mechanical properties of three joint sets [24, 25].

3. discrete element method

In this study, fracturing in a limestone environment due to propagate blast wave has been simulated in a granular form by PFC2D which is based on DEM. A solid is simulated as a collection of rigid disk particles (discrete elements) together using this code. Also, in order to apply boundary conditions, some rigid moveable walls are located around the assembled particles; the very important behavior in PFC2D models is actions and interactions of particles and walls at points of contacts. In the case of external loading on models, the mentioned process continues until the induced internal forces at the contacts reach a balance. Those contacts, which are simulated by springs, are soft meaning the particles can penetrate each other (Fig. 2). The contact forces are measured by the force-displacement law using the spring stiffness. Also, motions and displacements of particles due to the contact forces are simulated by Newton's second law. This software uses an explicit algorithm to model mechanical behaviors of solids. The contacts, particle and wall displacements are updated at each calculating step of this algorithm. The time steps are considered small enough to avoid the turbulence and distribution of forces in DEM models. Fig. 2 shows the contact between two discrete elements which is modeled by two springs with normal stiffness (K^n) and shear stiffness (K^s) and rheometers. Rheometer (which have the viscoelastic behavior with a constant viscosity) gradually reduce and make zero the kinetic energy in the models with a static equilibrium [29, 30].

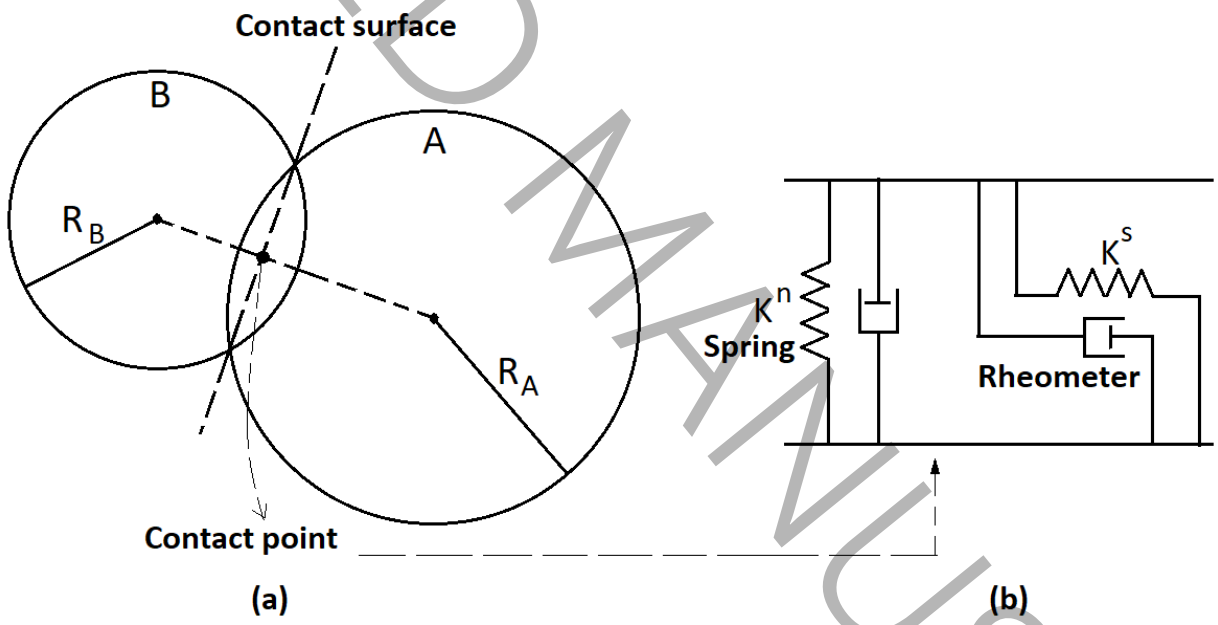

Fig. 2. a) Contact point between two particles, b) modeling contact with springs and rheometers [29,30].

According to Fig. 2, a new contact occurs when the distance between two particles is less than a critical value. By assuming that the behavior of the springs is linear, the contact force is decomposed into the normal and shear component on the contact surface. If the increase of relative displacement between particles in a time step is Δδ, for each time step [29,30]:

$$\begin{cases} F^n = \begin{cases} F_0^n + K^n \Delta\delta_n \rightarrow\rightarrow if\ \Delta\delta_n \le 0 \\ F_0^n \rightarrow\rightarrow if\ \Delta\delta_n > 0 \end{cases} \\ F^s = F_0^s - K^s \Delta\delta_s \end{cases} \quad (1)$$

F^n and F^s represent the normal and shear components of contact force, respectively. $\Delta\delta_n$ and $\Delta\delta_s$ denote the normal and shear components of increase rate in relative displacements between particles, respectively. The parameters with a zero index are equal to corresponding values at the end of previous time step. Properties that define the behavior of particles (such as density) and contacts (such as stiffness and coefficient of friction between particles when they slide on each other) are called micro-mechanical parameters, which are the required input values for the software [29,30]:

$$\begin{cases} K^n = AE/L \rightarrow\rightarrow\rightarrow A = 2r \\ K^s = \alpha K^n \end{cases} \tag{2}$$

$$\begin{aligned} r &= \min(R^A, R^B) \rightarrow\rightarrow contact \quad of \quad particle - particle \\ r &= radius \quad of \quad particle \rightarrow\rightarrow contact \quad of \quad particle - wall \\ L &= R^A + R^B \rightarrow\rightarrow contact \quad of \quad particle - particle \\ L &= radius \quad of \quad particle \rightarrow\rightarrow contact \quad of \quad particle - wall \end{aligned} \tag{3}$$

Where α and E are a constant value and Young's modulus of contact, respectively [27, 28].

Furthermore, a kind of bond can be defined at the contact point between two particles which causes the model to have mechanical behaviors similar to cementitious materials. The bond is simulated by springs that are parallel to the springs modeling the contact (Fig. 3). The motion of two discrete elements relative to each other creates force ($\overline{F}$) and bending moment ($\overline{M}$) in the bond: $\overline{F}$ is decomposed into normal ($\overline{F}^n$) and shear ($\overline{F}^s$) component on the contact surface [29,30].

$$\begin{cases} \overline{F^n} = \overline{F_0^n} + \overline{K^n}\,\overline{A}\Delta\delta_n \\ \overline{F^s} = \overline{F_0^s} - \overline{K^s}\,\overline{A}\Delta\delta_s \\ \overline{M} = \overline{M_0} - \overline{K^n}\,\overline{I}\Delta\theta \end{cases} \tag{4}$$

Where $\overline{K}^n$ and $\overline{K}^s$ are normal and shear stiffness of springs modeling the bonds, respectively. $\Delta\theta$ represents the relative rotation of the particles. $\overline{A}$ and $\overline{I}$ are the section area and the inertia moment of bond, respectively [29, 30].

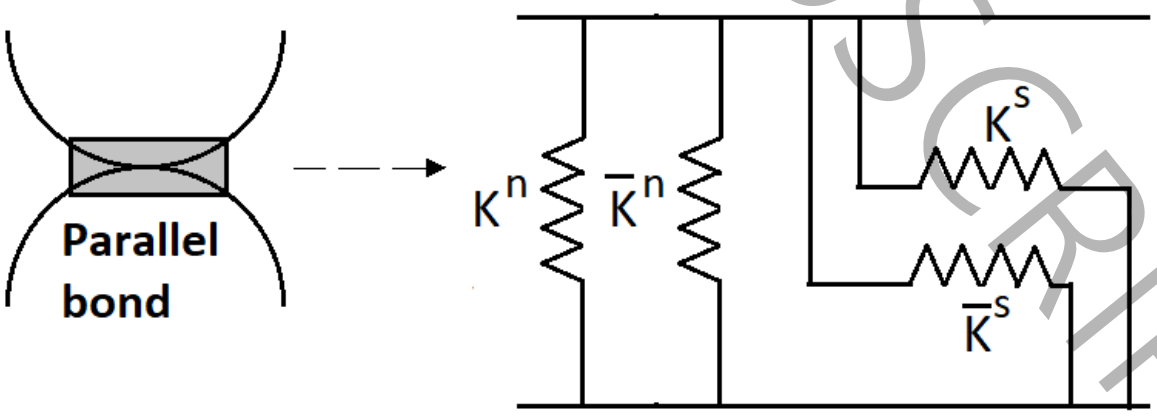

Fig. 3. A parallel bond between two particles [29, 30].

Finally, the maximum normal (σ_{max}) and shear stress (τ_{max}) created in the bond are measured as follows. If the stresses are greater than the corresponding resistances, a failure will occur and a crack will be formed [29, 30].

$$\begin{cases} \sigma_{\max} = \left(\left\|\overline{F^n} / \overline{A}\right\|\right) + \left(\left\|\overline{M}\right\| \overline{R} / \overline{I}\right) \\ \tau_{\max} = \left\|\overline{F^s}\right\| / \overline{A} \end{cases} \quad (5)$$

To simulate a continuous environment, the macro-mechanical properties of the environment can be obtained directly from experimental measurements. However, PFC2D analyzes a DEM model using the mentioned properties called micro-mechanical. It is impossible to measure micro-mechanical parameters of a solid by laboratory and in-situ tests. So in this study, the micro properties of studied limestone have been obtained by plane strain simulating the uniaxial compressive test as shown in Fig. 4; a rectangular specimen with a diameter of 54 mm and a height of 110 mm was created using the assembly of 5973 disc-shaped elements with radii of 0.5 to 1 mm. Some accidental values were defined as inputted-micro properties for the model and the test was carried out, then the values have been changed until the obtained results matched the properties estimated experimentally (Table 1). Furthermore, in order to ensure the accuracy of obtained micro-parameters, the standard Brazilian test was simulated as shown in Fig. 5. The determined tensile strength was equal to 4.81 MPa that is close to the experimental value (Table 1).

Table 3 gives the calculated micro-mechanical properties for limestone specimen used here for modeling the explosive process in the studied limestone.

Property	
Density	2500 Kg/m^3
Young's modulus of contact	54 GPa
Ratio of normal to shear stiffness of contact	1
Young's modulus of bond	54 GPa
Ratio of normal to shear stiffness of bond	1
Tensile strength of bond	4.9 MPa
Shear strength of bond	8 MPa
frictional coefficient between two particles	0.7

Table 3. Micro-mechanical properties of limestone obtained from DEM model.

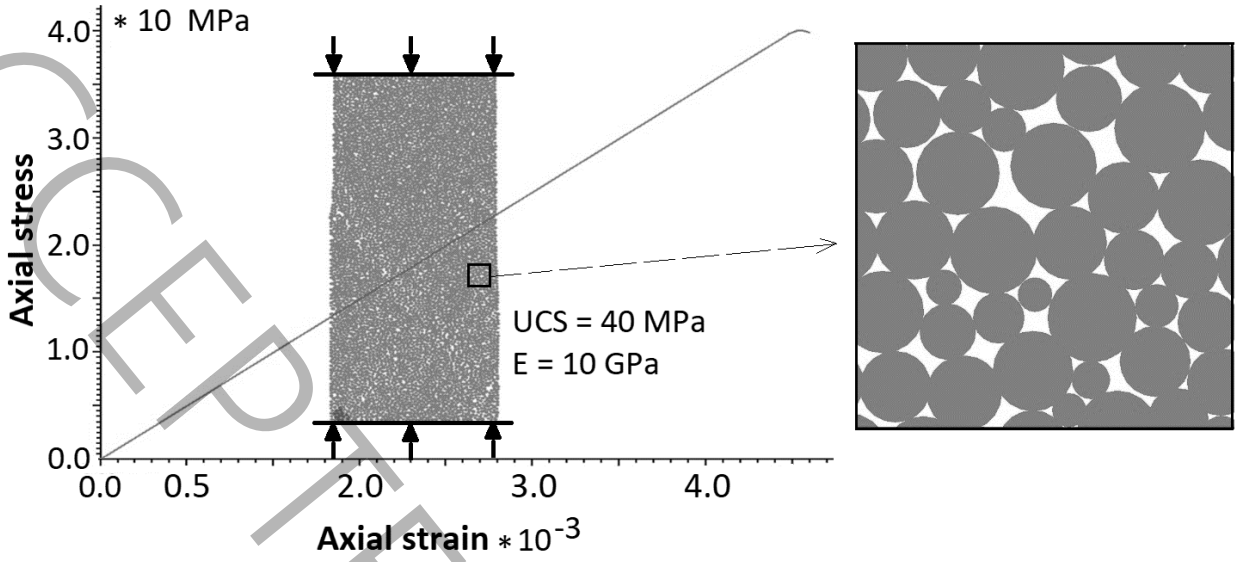

Fig. 4. DEM model of applied compressive test to limestone.

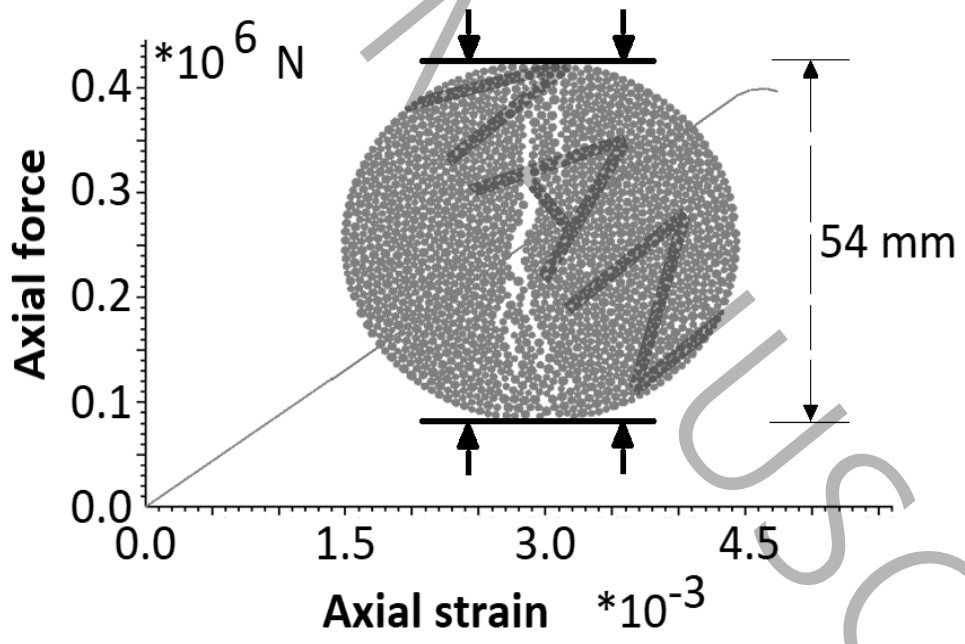

Fig. 5. DEM model of applied Brazilian test to limestone produced by 2298 bonded particles.

4. DEM model of stress wave propagation

In order to simulate the explosive-stress-wave propagation, it assumed that the assembly of bonded stiff particles is equivalent to a continuous environment. The limestone was simulated by 93031 disc-shaped and bonded particles with radii of 0.5 to 1 mm. The micro-mechanical parameters shown in Table 3 were used for defining the properties of the modeled-studied rock (Fig. 6). The pressure of blasting was applied to inner walls of six excavated holes in limestone during a few hundredths of a second, causing stress waves to propagate along the particles that are in contact with each other (Fig. 7). As mentioned in the last section, when the stresses induced in the bonds exceeded their strength, they broke and cracks were produced. These cracks and joint sets dropped the wave energy [26]. As shown in Fig. 6, B is the smallest distance between the hole row and the free surface (i.e. burden). S is and the distance between the holes (i.e. spacing) [7].

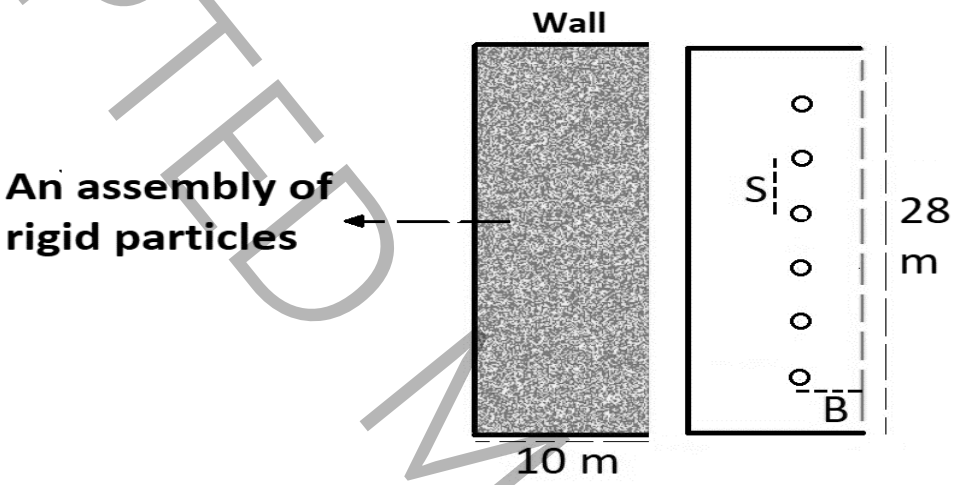

Fig. 6. DEM model of a non-jointed rocky environment including 6 explosive holes.

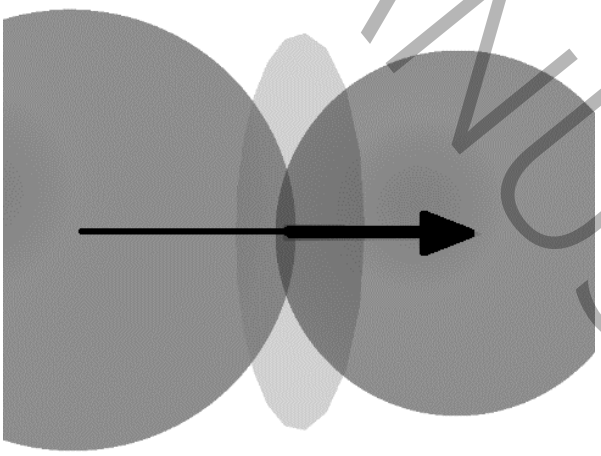

Fig. 7. transferring stress wave between to particles that are in contact with each other [29, 30].

The maximum pressure (P_{max}) produced from an explosive material was calculated by the following formula; it carried out on the inner body of hole due to explosion [31]:

$$P_{\max} = 0.125\rho_e \left(V_e\right)^2 \quad (6)$$

Where ρ_e and V_e are the density of explosive material and blast velocity, respectively. The explosive material using in Angooran mine is ANFO with 820 Kg/m^3 in density and 3100 m/s in blast velocity [7], so the maximum blast pressure applied to the inner walls of holes was equal to 1 GPa.

4.1. **Continues-rocky environment**

To simulate stress wave propagation, the blast pressure was applied to the inner body of six holes shown in Fig. 6. The pressure increased gradually from 0 (at 0 second) to 1 GPa at 0.45 seconds, then it decreased gradually from 1 GPa to 0. Fig. 8 shows the distribution of cracks in the DEM model with the different patterns of holes. The results showed that producing the large pieces of rocks and the back-break processes increased by making the burden larger. It wasted a large part of explosive energy in growing back-break rates and ground vibration processes [7]. Also, raising the spacing caused the back-break and number of large rocky pieces to increase. In contrast, decreasing the burden remarkably increased the crushing rock rates and powdered areas.

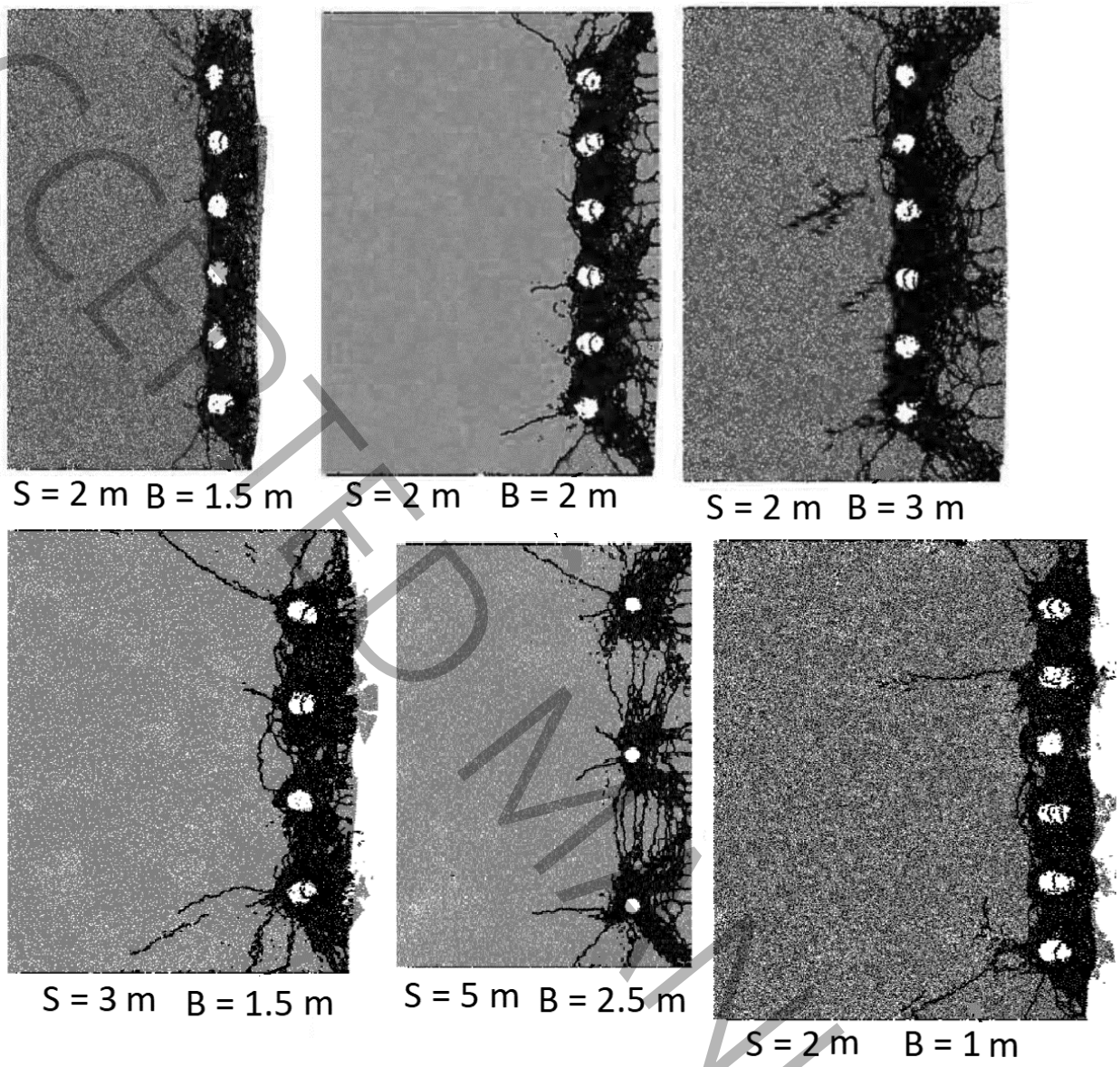

Fig. 8. DEM models of crack distribution in non-jointed limestone environment with different blast patterns (cracks are shown with black color).

4.2. **Jointed rocky environment**

To investigate effects of joints on rock fracturing, the joint sets, whose parameters were given in Table 2, have been simulated using discrete fracture network (DFN) method as shown in Fig. 9. DFN model is a set of statistical distribution of cracks with geometrical characteristics such as fracture sizes, orientations and positions combined with the rocky environment [26]. The blast pressure was applied to the inner body of holes according to the method mentioned above. The crack distributions of the jointed limestone environment with B = 1 m was approximately similar to the fractures of the non-jointed environment with B=1.5 m. In other words, the existence of joints decreased the energy of stress wave propagation. When the wave reached the empty space between the joint surfaces, it lost a large part of its energy and the wave passed from the joints could not break limestone well and large pieces of rock were created. Also, the

reflected wave increased the back-break areas. So, the burden of explosive holes in a jointed limestone should reduce relative to those in the jointed rock [32, 33].

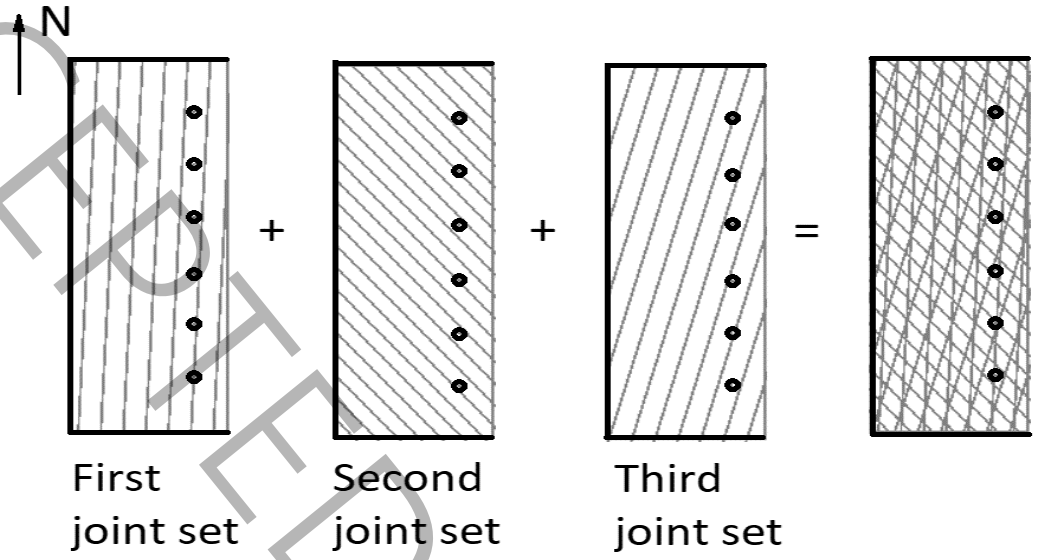

Fig. 9. DEM model of limestone environment including three joint sets and 6 explosive holes.

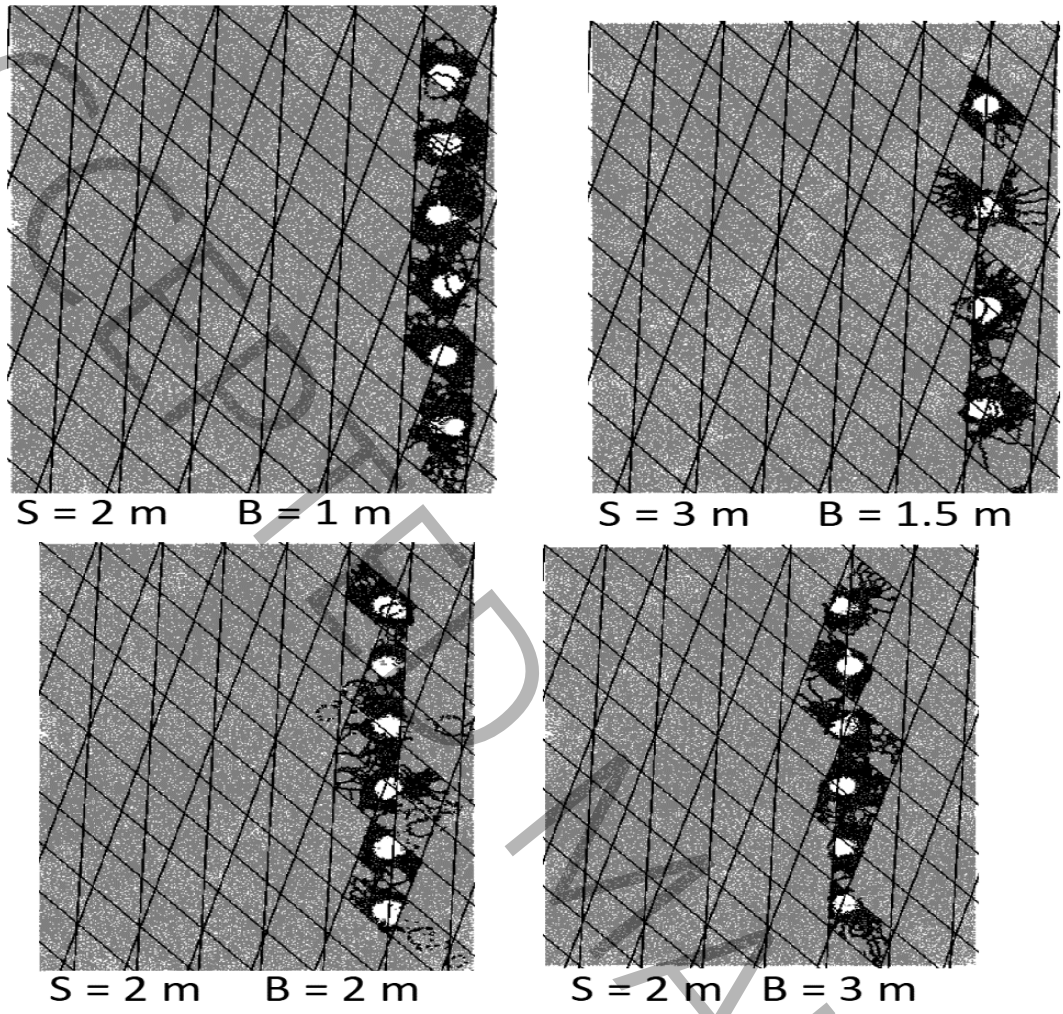

Fig. 10. DEM models of crack distribution in jointed limestone environment with different blast patterns (cracks are shown with black color).

Based on geological characters of Angooran mine, the optimum blast pattern in the east jointed area of the mine is B=1 m and S=2 m, because the large pieces of rock considerably decreased. Also, too many fractures and around each hole showed the powered areas (Fig. 8 and 10).

4.3. **Validating DEM model of explosion**

Distributing many fractures around the blast hole and creating radial cracks are the important result during the explosion. Several researches have showed different broken areas and cracks created close to crater of a explosive hole. Fig. 11 shows the powder area and radial cracks after blowing up a hole in an experimental test and the DEM model developed in this study. Also previous studies showed when blasting stress waves reach the free surface, reflection tensile waves are generated and cause tensile fractures that were approximately similar to the results obtained in this study [32, 33].

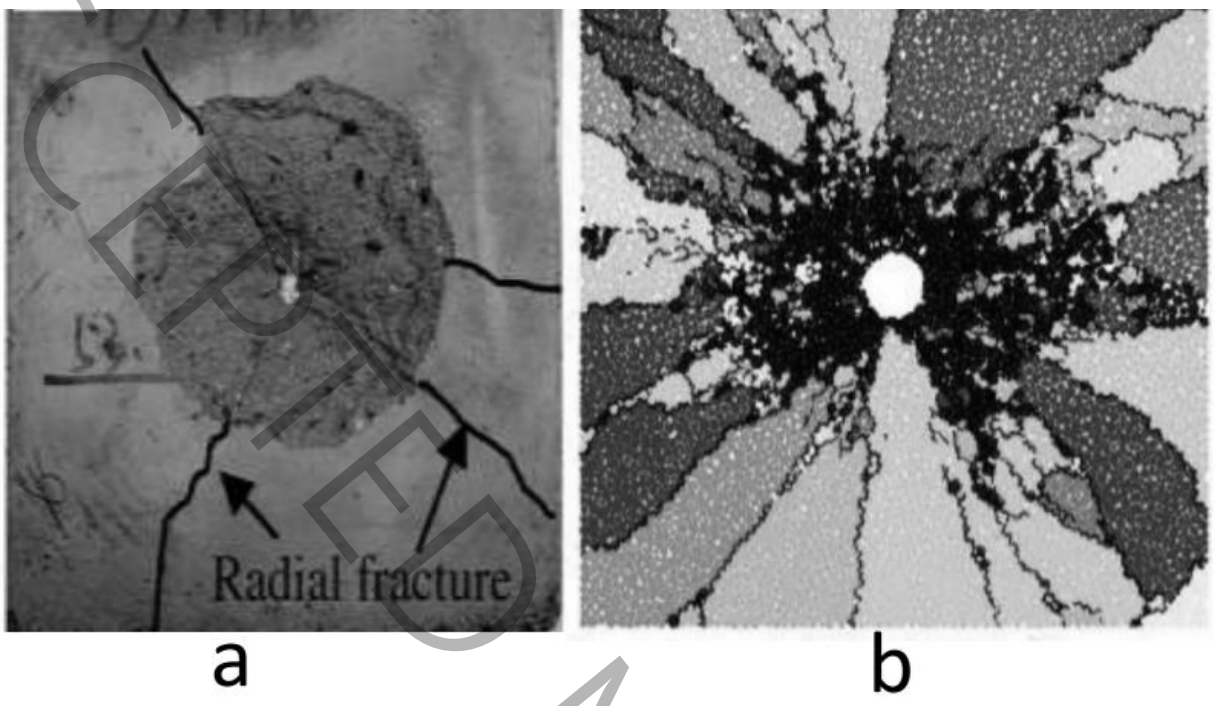

Fig. 11. Powdered area and radial fracture around an explosive hole a) tested experimentally [33] and b) in a developed DEM model in this study (cracks are shown with black color).

5. Conclusion

(1) The effect of rock joints on the propagation of stress wave due to the explosion of six holes in limestone was studied here by the discrete element method (DEM). For this purpose, a non-jointed and jointed limestone environment were modeled using the particle flow code in two dimensions (PFC2D); the condition of model was assumed as the plane strain. The results obtained from simulating wave propagation in the non-jointed rock showed that producing large pieces of rocks and back-break processes increased by making the burden larger, causing to waste a large part of explosive energy. However, decreasing B remarkably increased the degree of crushing rock, causing to produce more powdered materials. Furthermore, large number of cracks around the holes showed that the powdered areas started to develop by the propagating the blast-stress wave.

(2) Simulating blast pressure carried out on jointed limestone confirmed when the wave reached the empty space between the joint surfaces, it lost a large part of its energy and the wave passed the joints could not break the rock well and the rocky large pieces were produced. Furthermore, the reflected stress wave increased the back-break areas. So, the burden of explosive holes in a jointed limestone should reduce relative to those in the jointed rock.

(3) Using DEM models, the optimum pattern of blast holes for jointed limestone environment, where is located in the east area of Angooran mine, was B=1 and S=2 m. Also, comparing the results obtained from DEM model of blasting holes with accurate experimental data showed that the discrete element method was an appropriate method to simulate the rock fracturing by the blast-stress wave propagation.

References

[1] ECJ Gan, A. R. (2024). "A Blast propagation and hazard mapping outside coal mine tunnels and shafts." Tunnel Undergro Spac Tec 148.

[2] MS Bahraini, I. A. (2024). "A novel intelligent stereo vision approach for blast-induced fragmentation size distribution: Case study at Golgohar open-pit mine, Iran." Miner Eng 215.

[3] Hagan, T. (1979). "Rock breakage by explosive." Acta Astrona 6: 329-340.

[4] C Drover, E. V., I Onederra (2018). "Face destressing blast design for hard rock tunnelling at great depth." Tunnel Undergro Spac Tec 80: 257-268.

[5] LF Trivino, B. M. (2015). "Assessment of crack initiation and propagation in rock from explosion-induced stress waves and gas expansion by cross-hole seismometry and FEM–DEM method." Int J Rock Mech Mini Sci 77: 287-299.

[6] B Satyabrata, D. K. (2024). "Prediction of Backbreak in Surface Production Blasting Using 3-Dimensional Finite Element Modeling and 3-Dimensional Nearfield Vibration Modeling." Min Metallu & Explor.

[7] CL Jimeno, E. J., FJA Carcedo (1995). Drilling and blasting of rocks. London, Taylor & Francis.

[8] L Liu, P. K. (1977). "A numerical study of the stress of short delays on rock fragmentation." Int J Rock Mech Mini Sci 34(5): 817-835

[9] M Monjezi, H. D. (2008). "Evaluation of effect of blasting pattern parameters on back break using neural networks." Int J Rock Mech Mini Sci 45(8): 1446-1453.

[10] X Li, Z. Z., M Wang, D Xiao, Y Shu, S Deng (2021). "Fracture mechanism of rock around a tunnel-shaped cavity with interconnected cracks under blasting stress waves." Int J Impa Eng 157.

[11] J Zhang, Z. C., K Shao (2024). "Numerical investigation on optimal blasting parameters of tunnel face in granite rock." Simula Model Pract Theo 130.

[12] Z Wang, Q. L., W Chen, H Hao, L Li (2024). "Fragment prediction of reinforced concrete wall under close-in explosion using Fragment Graph Network (FGN)." Compu Struc 305.

[13] EF Salmi, E. S. (2021). "A review of the methods to incorporate the geological and geotechnical characteristics of rock masses in blastability assessments for selective blast design." Eng Geolog 281.

[14] C Mao, H. C., X Xie, C Liu, S Wang, J Jia, J Du, Z Lv, J Luo, Y Liu (2024). "Microstructure and mechanical-property evolution of the explosive welding joint from the same RAFM steels under explosive welding and post-weld heat treatment." Mater Sci Eng part A 918.

[15] P Cai, Z. X., Y Liu, X Chen, W Qi, L Liu (2024). "Weakly confined slotted cartridge blasting in jointed rock mass." Theo Appl Frac Mech part A 134.

[16] SH Cho, K. K. (2004). "Influence of the applied pressure waveform on the dynamic fracture processes in rock." Int J Rock Mech Mini Sci 41(5): 771-784.

[17] P Niu, S. W., G Feng, Y Xiao, B He, Z Yao, L Hu, Z Wu (2024). "Influence of stress and geology on the most prone time of rockburst in drilling and blasting tunnel: 25 tunnel cases." Eng Geo 340.

[18] P Wang, L. W., Y Wang (2023). "Influence of material heterogeneity on the blast-induced crack initiation and propagation in brittle rock." Comput Geotech 155.

[19] P Zhang, L. Y., D Man, N Liu, P Wei, Z Sui, Y Liu (2024). "Explosive stress wave propagation and fracture characteristics of rock-like materials with weak filling defects." Eng Frac Mech 308.

[20] S Mohd, T. S. (2015). "Numerical assessment of spacing–burden ratio to effective utilization of explosive energy." Int J Rock Mech Mini Sci 25: 291-297.

[21] Khademian, A. (2024). "Optimization of blasting patterns in Esfordi phosphate mine using hybrid analysis of data envelopment analysis and multi-criteria decision making." Eng Appl Artif Intel part A 133.

[22] X Jiang, Y. X., F Kong, H Gong, Y Fu, W Zhang (2024). "Dynamic responses and damage mechanism of rock with discontinuity subjected to confining stresses and blasting loads." Int J Imp Eng 172.

[23] GW Ma, X. A. (2008). "Numerical simulation of blasting-induced rock fractures." Int J Rock Mech Mini Sci 45(6): 966-975.

[24] J Ding, J. Y., Z Ye, Z Leng, C Zhou (2024). "Numerical study on rock blasting assisted by in-situ stress redistribution." Tunnel Under Spa Tech 153.

[25] W Jianxiu, Y. Y., K Esmaieli (2018). "Numerical simulation of rock blasting damage based on laboratory-scale experiments." J Geophysi Eng 15(6): 2399-2417.

[26] X Huang, S. Q., A Williams, Y Zou, B Zheng (2015). "Numerical simulation of stress wave propagating through filled joints by particle model." Int J Soli Struc 69-79: 23-33.

[27] SS Behbahani, P. M., K Ahangari, K Goshtasbi K (2013). "Unloading scheme of Angooran mine slope by discrete element modeling." Int J Rock Mech Mini Sci 64: 220-227.

[28] E Yaghoubi, M. S., P Maarefvand (2017). "Slope stability analysis and evaluation of further major failure in Angooran open-pit mine." J Analyt Numer Meth Mini Eng 6(12): 33-45.

[29] DO Potyondy, P. C. (2004). "A bonded-particle model for rock." Int J Rock Mech Mini Sci 41: 1329-1364.

[30] L Jing, O. S. (2007). Fundamentals of discrete element methods for rock engineering, theory and applications. Amesterdam, Elsevier.

[31] Aladejare, A. (2020). "Evaluation of empirical estimation of uniaxial compressive strength of rock using measurements from index and physical tests." J Rock Mech Geolog Eng 12(2): 256-268.

[32] Z Ye, J. Y., M Chen, C Yao, X Zhang, Y Ma, C Zhou (2024). "Difference in rock-breaking characteristics between water-coupling blasting and air-coupling blasting." Int J Roc Mech Min Sci 183.

[33] F Zhang, J. P., Z Qiu, Q Chen, Y Li, J Liu (2017). "Rock-like brittle material fragmentation under coupled static stress and spherical charge explosion." Eng Geolog **220**: 266-273.